ANL/TD/CP--85126
Conf-9409107--12

Neutronic Study on Conversion of SAFARI-1 to LEU Silicide Fuel*

G. Ball
Atomic Energy Corporation of South Africa Limited
Pretoria, South Africa

R. Pond, N. Hanan and J. Matos
Argonne National Laboratory
Argonne, Illinois 60439-4841 USA

To be presented at the
1994 International Meeting on
Reduced Enrichment for Research and Test Reactors

September 18-23, 1994
Williamsburg, Virginia USA

*Work supported by the U.S. Department of Energy
Office of Nonproliferation and National Security
under Contract No. W-31-109-38-ENG

DISCLAIMER

Portions of this document may be illegible in electronic image products. Images are produced from the best available original document.

Neutronic Study on Conversion of SAFARI-1 to LEU Silicide Fuel

G. Ball
Atomic Energy Corporation of South Africa Limited
Pretoria, South Africa

R. Pond, N. Hanan and J. Matos
Argonne National Laboratory
Argonne, Illinois 60439-4841, USA

ABSTRACT

This paper marks the initial study into the technical and economic feasibility of converting the SAFARI-1 reactor in South Africa to LEU silicide fuel. Several MTR assembly geometries and LEU uranium densities have been studied and compared with MEU and HEU fuels. Two factors of primary importance for conversion of SAFARI-1 to LEU fuel are the economy of the fuel cycle and the performance of the incore and excore irradiation positions.

INTRODUCTION

The Atomic Energy Corporation of South Africa Ltd (AEC) supports the principles of the Reduced Enrichment for Research and Test Reactor (RERTR) Program and its nonproliferation goal of reducing or eliminating international trade in highly enriched uranium. After exploratory discussions a joint study into the technical and economic feasibility of conversion of the SAFARI-1 Reactor was initiated in September 1993 with the signing of a protocol agreement between the RERTR Program at Argonne National Laboratory (ANL), the United States Department of Energy and the AEC.

This paper presents the results of the first phase of the work, namely the neutronic study. Subsequent phases will include safety studies and economic issues. As the AEC is currently undergoing a transition towards a more commercially oriented organisation the economic impact of any conversion is of primary concern. The fuel cycle and the neutron flux spectrum and the flux level in the incore and excore irradiation positions will feature prominently in the final conversion decision.

In this paper the results of core performance as a function of various enrichments, loadings and assembly geometries are reported. Proven fuel assembly designs and loadings with minimum changes to the current core configuration have been utilised.

SAFARI-1 CHARACTERISTICS AND UTILISATION

The SAFARI-1 reactor is a 20MW pool-type materials testing reactor operated by the AEC at its Pelindaba site near Pretoria, South Africa. Since its commissioning in 1965, the reactor has operated with an exemplary safety record. It is supported by the infrastructure of the AEC which includes a fuel fabrication plant, hot cell facilities, isotope production centre, radioactive waste disposal site and a theoretical reactor physics support group.

The reactor is located in a large pool with easy access to both incore and excore irradiation positions. An 8x9 grid houses 28 fuel assemblies, 5 control rods, 1 regulating rod, the incore irradiation facilities and the reflector elements. The core is fuelled with the 19-plate MTR-type fuel elements shown in Figure 1. The control rods are comprised of a 15 plate fuel follower section (shown in Figure 2) beneath a cadmium absorber section.

The reactor originally was fuelled with 90 wt% enriched uranium-aluminium alloy fuel (HEU) but was converted to a 45 wt% uranium-aluminium alloy (MEU) during the early 1980's. Due to the higher scrap rate in the manufacturing process of our MEU fuel and the availability of HEU in South Africa it was recently decided to return to the manufacture and use of HEU fuel assemblies for economic reasons. The first of the HEU assemblies will be loaded into the core prior to the end of 1994. This decision was made prior to the commencement of this joint study on the feasibility of converting SAFARI-1 to use low enriched uranium silicide fuel.

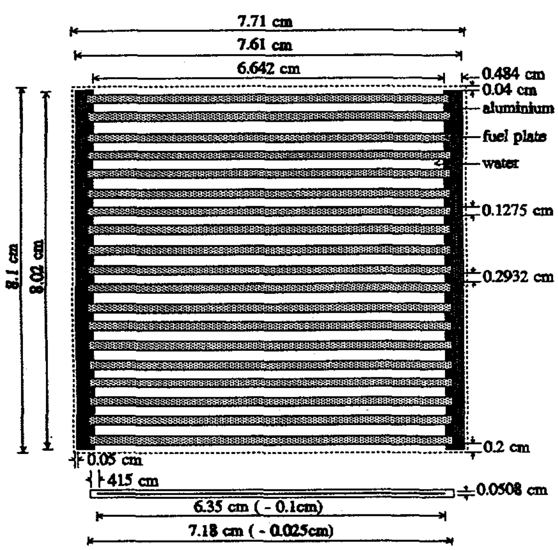

Figure 1: SAFARI-1 Fuel Assembly

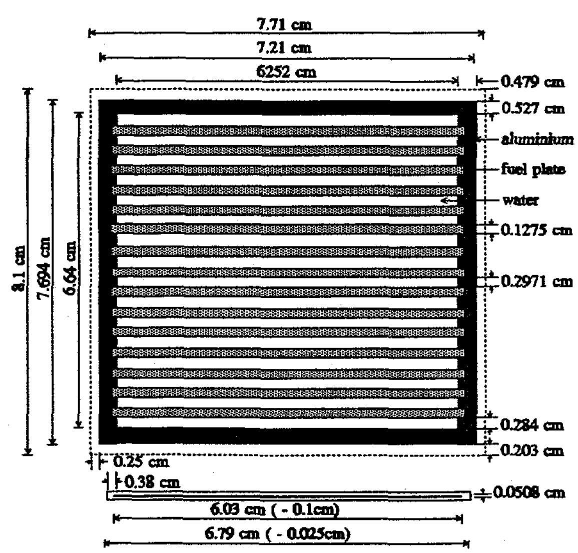

Figure 2: SAFARI-1 Follower Assembly

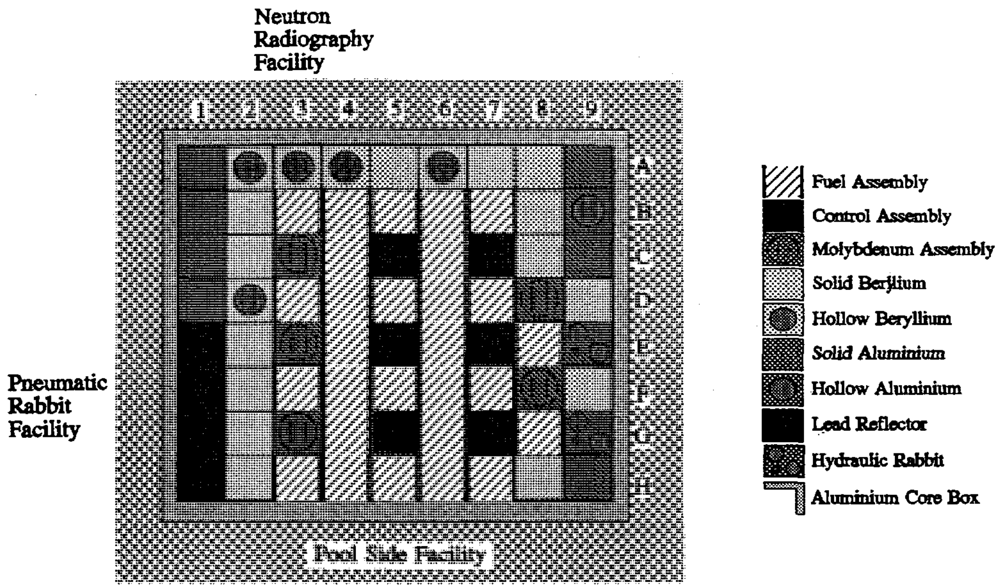

Figure 3: SAFARI-1 Core

SAFARI-1 has several incore irradiation positions, some of which can be loaded while the reactor is at power. Most of these positions are reserved for molybdenum production. All the South African Mo^{99} requirements have been met since June 1993 and a program for the large scale production of molybdenum is in place. Various other radioactive isotopes for medical and industrial applications are also produced.

The reactor vessel is cylindrical in shape except for one flattened side which is also the wall of the rectangular core box adjacent to the pool side facility. This large excore pool side facility allows irradiations to be performed in relatively high neutron fluxes since it is directly adjacent to the fuel elements. Irradiations in the pool side can be performed as close as 3.5cm from the fuel. The pool side houses our automated silicon irradiation facility (SILIRAD)[1] which has a current annual capacity of 5 tons at a reactor power level of 10MW. Gemstone irradiations are also performed in the pool side.

The reactor is also equipped with a number of beam tubes, one of which services our neutron radiography facility, while hydraulic and pneumatic rabbit facilities provide for the irradiation of various material samples.

CALCULATIONAL MODEL

The computer code WIMSD4m[2] was used to generate burnup dependent microscopic cross sections in six energy groups using slab geometry representations for the fuel and control rod follower materials. The fuel cross sections for the standard fuel and follower were generated with a three-region cell consisting of fuel, clad and moderator while the fuel assembly side plates were modelled by including an extra region containing a volume weighted mixture of water and aluminium. Microscopic cross sections for the irradiation positions and the beryllium, aluminium and lead reflector regions were also generated with WIMSD4m using slab models. The reflector assemblies and irradiation positions have been represented as closely as possible in their true environment (within the limitations of the WIMSD4m one-dimensional model).

The core neutronics and burn-up calculations were performed in three dimensions using the REBUS code system[3] and the DIF3D[4] diffusion theory neutronics code. A detailed Monte Carlo model using the MCNP[5] code was used for benchmarking the accuracy of the diffusion theory model results.

The active fuel and side plate regions have been modelled separately in the diffusion theory calculations. Elements with cylindrical holes were modelled exactly in MCNP and as volume equivalent square holes in DIF3D. A substantial effort was made both in the diffusion theory and Monte Carlo models to accurately represent the key irradiation positions of economic interest. Average thermal fluxes and thermal-to-total ratios have been calculated for each irradiation facility to characterise these positions as a function of the different fuels.

In the pool side, average fluxes and flux-ratios have been calculated in a horizontal region 12 cm from and parallel to the core face at the axial core centre. This position coincides with the centre of the SILIRAD position when it is in operation. The neutron radiography beam tube itself was not modelled but average fluxes and flux ratios calculated in water adjacent to the core box in the vicinity of the beam tube.

The five molybdenum irradiation positions in the core each consist of an aluminium element with a cylindrical hole filled with water into which the target plates are inserted. Fluxes and flux ratios, in water in the positions where the target plates are placed, averaged over all five positions have been calculated. The hydraulic rabbit was modelled homogeneously in both DIF3D and MCNP and the fluxes and flux ratios averaged over the four tubes of the rabbit facility. And lastly, the excore pneumatic rabbits themselves have not been modelled but average fluxes and flux ratios calculated in the water adjacent to the core box in the vicinity of the pneumatic rabbit facility.

MODEL VALIDATION

Initially, comparisons of thermal fluxes and thermal-to-total flux ratios in five irradiation locations were made between DIF3D and MCNP for an all-fresh core with control rods withdrawn. Volume averaged fluxes and flux ratios over each irradiation facility described previously were calculated. Table 1 shows the percentage differences in the flux and flux ratios for each facility.

The smaller differences between the two codes for the hydraulic rabbit is due to its homogeneous treatment by both codes thus eliminating modelling differences with respect to geometrical effects. Notice also that although there is an 8.6% difference in the absolute value of the thermal flux in the pool, side the flux ratio is practically the same.

Table 1: Thermal Flux and Thermal-to-Total Flux Ratios for Fresh Core
(DIF3D percentage differences from MCNP)

Position	Thermal flux (% difference)	Thermal-to-total ratio (% difference)
Pool Side	8.6	0.5
Neutron Radiography Beam Tube	-9.0	-5.9
Molybdenum	-4.8	-6.1
Hydraulic Rabbit	0.5	-1.4
Pneumatic Rabbit Vicinity	-4.9	-7.0

The MCNP results had an uncertainty of ±2%.

Experimentally determined control rod worths were also used to validate the Monte Carlo results. Control rod worths for a fresh and burned core are given in Table 2 below.

Table 2: Control Rod Worths for MEU core

	Fresh Core ($)	Actual Core ($)
Measured	-	32.2
MCNP	31.3 ± 0.3	32.5 ± 0.3
DIF3D	32.8	34.3

The good agreement of the rod worth calculated with diffusion theory is due to the use of internal black absorber boundary conditions in the DIF3D code for the cadmium absorber in the control rods. Without the application of these internal absorber conditions the diffusion calculations underestimate the rod worth by as much as 14%.

BURNUP CHARACTERISTICS FOR EQUILIBRIUM CORES

An equilibrium cycle was defined to represent the current average SAFARI-1 operational procedures as closely as possible. This was achieved by examining the actual reloads performed during the past year and defining an average reload pattern based on these data. The fuel shuffle paths are given in the appendix. The resulting assembly U^{235} mass distribution in the calculated equilibrium core was then compared with the average of the U^{235} masses in each core position estimated from operational data over the past year. The equilibrium core cycle length and discharge burnups of the spent fuel assemblies is in good agreement with operational data.

Equilibrium core studies have been performed for 45 wt% enriched uranium-aluminium alloy fuel (MEU) with a U^{235} loading of 225g per standard fuel assembly (SFE), for 90 wt% enriched uranium-aluminium alloy fuel (HEU) with U^{235} loadings varying from 200g to 300g per SFE and for 19.75 wt% U_3Si_2-Al (LEU) with loadings varying from 225g U^{235} to 485g U^{235} per SFE. HEU alloy and LEU silicide fuel assemblies that contain less than 340 g of U^{235} have the standard 19-plate fuel geometry with 0.051 cm thick meat. LEU silicide fuel assemblies that contain more than 340g of U^{235} have 18 fuel plates with 0.076 cm thick fuel meat. These 18-plate assemblies allow the same U^{235} loadings per assembly with reduced uranium densities thereby decreasing the possible scrap rate in the manufacturing process and allowing the flexibility of increasing the U^{235} loadings per fuel assembly further.

In all equilibrium core cases the End-of-Cycle (EOC) core excess reactivity has been fixed at the average excess reactivity of several recent cores with control rods fully withdrawn. With the control rods fully withdrawn, the follower fuel coincides exactly with the top and bottom of the active fuel in the core while the bottom of the cadmium is 3.85 cm above the top of the fuel. This being the case and in order to shorten computing times, this model was simplified by neglecting the control rods and assuming symmetry across the axial core centre line. Calculations showed that the effect of neglecting the control rods and modelling the core symmetrically for these cases is minimal and is adequate for these comparative purposes.

The reload pattern described above was applied to equilibrium core calculations with HEU, MEU and LEU fuels. Table 3 summarizes the cycle lengths, percentage burnup of U^{235} in the fuel and followers on discharge and the total number of assemblies (including followers) used per year.

Table 3: Fuel used Annually as Function of Assembly Type

Description	U density	Cycle Length	U^{235} Discharge Burnup (%)		Assemblies
	($g.cm^{-3}$)	(fpd)	Fuel	Follower	used pa[1]
MEU 225g, 19 plates	1.35	15.2	48.1	66.6	68
HEU 200g, 19 plates	0.61	12.6	45.4	63.5	82
HEU 250g, 19 plates	0.76	19.2	55.8	74.8	54
HEU 300g, 19 plates	0.92	26.7	65.1	83.8	40
LEU 225g, 19 plates	3.13	13.6	42.0	59.1	76
LEU 285g, 19 plates	3.97	22.3	53.7	72.5	47
LEU 340g, 19 plates	4.73	30.1	60.5	79.1	35
LEU 340g, 18 plates	3.34	28.5	57.4	76.2	37
LEU 400g, 18 plates	3.93	36.7	62.3	80.8	30
LEU 485g, 18 plates	4.76	48.2	67.1	84.9	23

(1) Based on a power level of 20MW and 294 effective full power days per annum.

The cycle lengths of the different fuels as a function of U^{235} content is presented graphically in Figure 4 below. Using the MEU as a basis for comparison it was noted that for the 19 fuel plate assemblies 3% less U^{235} is required to be loaded per HEU fuel assembly while 5% more U^{235} is required per LEU fuel assembly to match the current cycle lengths with MEU. This is due to different quantities of U^{238} in the fuels.

It was also noted that 3% more U^{235} is required in the LEU 18-plate assemblies (thicker fuel meat) than the LEU 19-plate assemblies to match the cycle length of the former fuel assemblies. The advantage however, is that a thicker fuel meat allows more U^{235} to be loaded per assembly.

The increased cycle lengths due to the higher uranium loadings shown in Figure 4 make increased uranium densities an attractive option to cut the fuel operating costs of the reactor. This is an important consideration that will be factored into the economic analysis.

Two additional equilibrium core calculations were performed with 340 grams of LEU loaded per assembly. The fuel assemblies used had 20 fuel plates with meat thicknesses of 0.076 cm and 23 plates with fuel meat thicknesses of 0.051 cm. The resulting cycle lengths, percentage burnup of U^{235} on discharge and total number of assemblies used per year for various assemblies loaded with 340 grams of LEU are given in Table 4 below. Due to the harder spectrum resulting from the use of these LEU 20 and 23 plate assemblies it requires approximately 3 to 4 more fuel assemblies per year to match the cycle length of the 19-plate LEU assemblies.

Table 4: Fuel used Annually for 340 g Loaded LEU Fuel

Description	U density	Cycle Length	U^{235} Discharge Burnup (%)		Assemblies
	(g.cm^{-3})	(fpd)	Fuel	Follower	used pa[(1)]
18 plates, 0.076 cm meat	3.34	28.5	57.4	76.2	37
19 plates, 0.051 cm meat	4.73	30.1	60.5	79.1	35
20 plates, 0.076 cm meat	3.00	27.0	54.6	72.7	39
23 plates, 0.051 cm meat	3.91	27.9	56.2	74.0	38

[(1)] Based on a power level of 20MW and 294 effective full power days per annum.

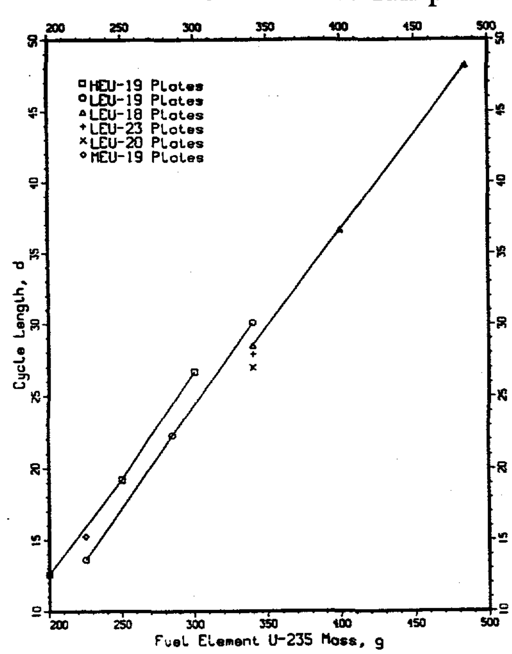

Figure 4: Cycle Length versus Fuel Type and Loading

FLUX AND SPECTRUM COMPARISONS FOR EQUILIBRIUM CORES

As mentioned previously, the neutron flux levels and neutron spectrum in the irradiation positions are of prime importance to the commercial products produced at SAFARI-1.

MEU fuel assemblies with 19 plates and 225 grams U^{235} are currently used in the SAFARI-1 core and as such have been used as the reference in comparing the effects of the other fuels on the flux level and spectrum. Comparisons of the thermal flux and thermal-to-total flux ratios have been made, in each of the irradiation positions mentioned previously, for the different fuels and are given in terms of the percentage differences from the current MEU core operation in the series of figures below.

Figure 5. THERMAL FLUX: POOL SIDE

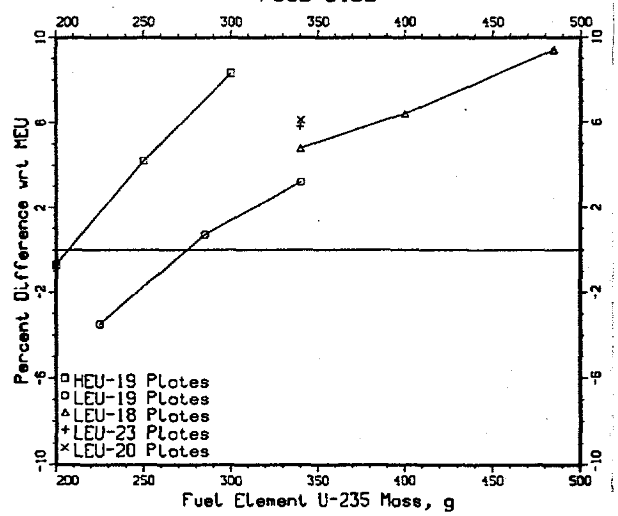

Figure 6. THERMAL-TO-TOTAL FLUX RATIO: POOL SIDE

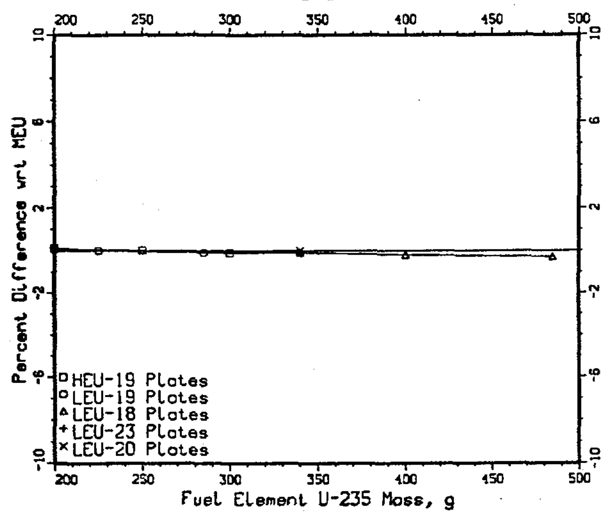

Figure 7. THERMAL FLUX: NEUTRON RADIOGRAPHY BEAM TUBE

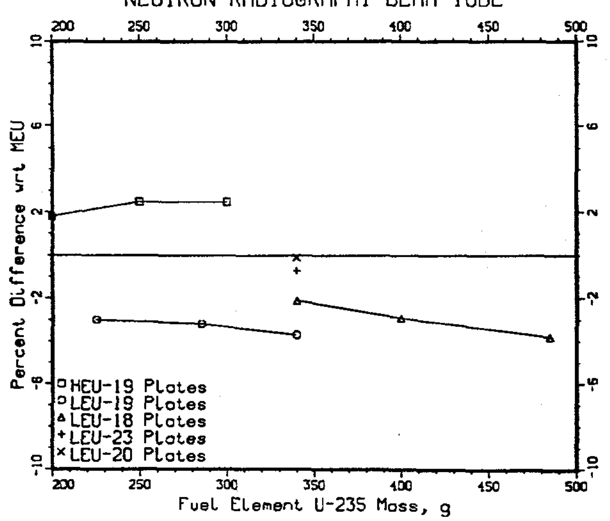

Figure 8. THERMAL-TO-TOTAL FLUX RATIO: NEUTRON RADIOGRAPHY BEAM TUBE

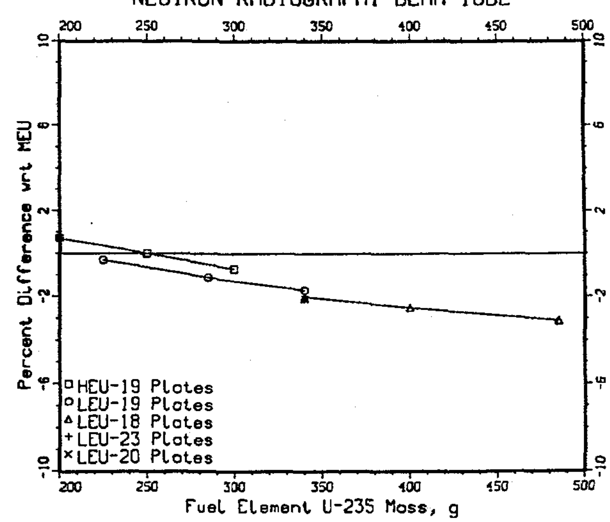

Figure 9. THERMAL FLUX:
MOLYBDENUM

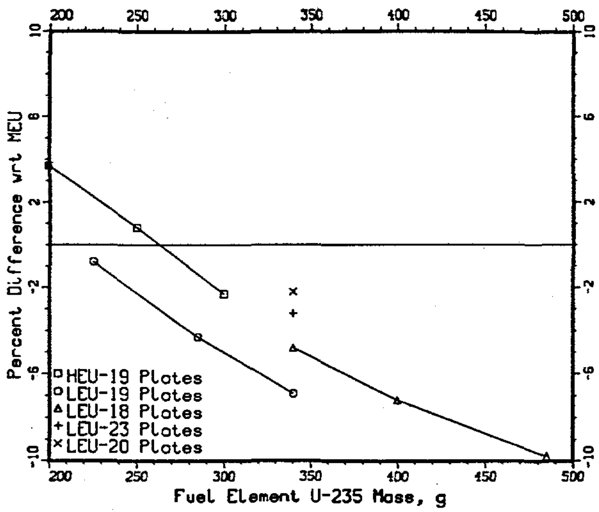

Figure 10. THERMAL-TO-TOTAL FLUX RATIO:
MOLYBDENUM

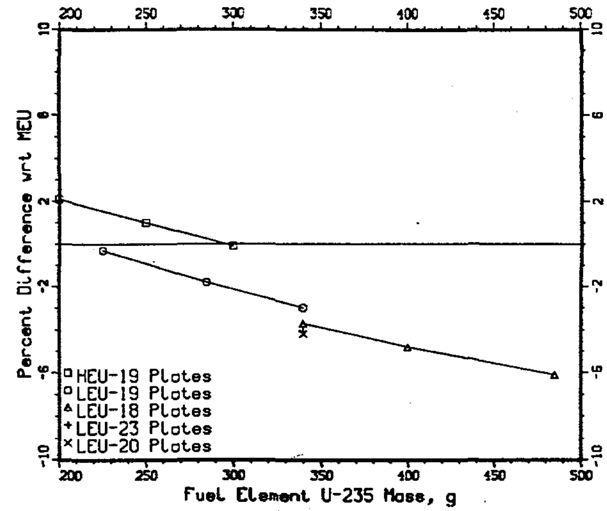

Figure 11. THERMAL FLUX:
HYDRAULIC RABBIT

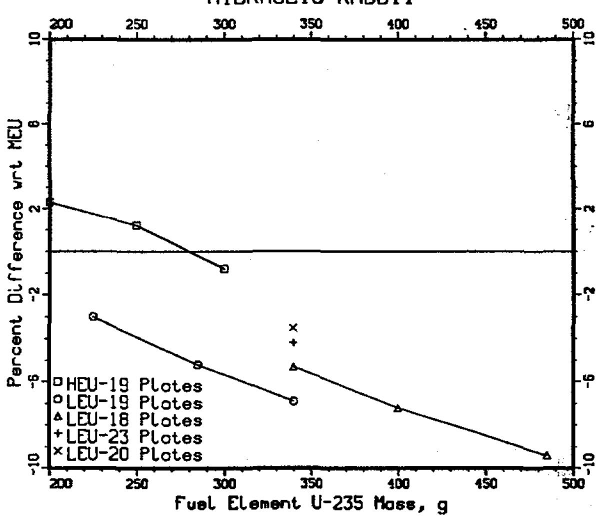

Figure 12. THERMAL-TO-TOTAL FLUX RATIO:
HYDRAULIC RABBIT

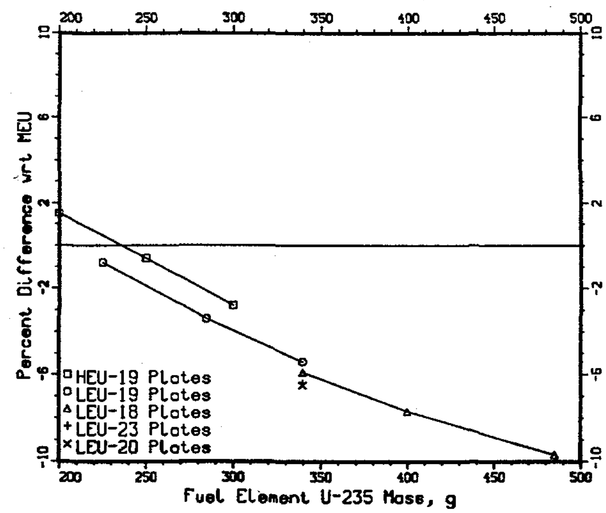

Figure 13. THERMAL FLUX:
PNEUMATIC RABBIT

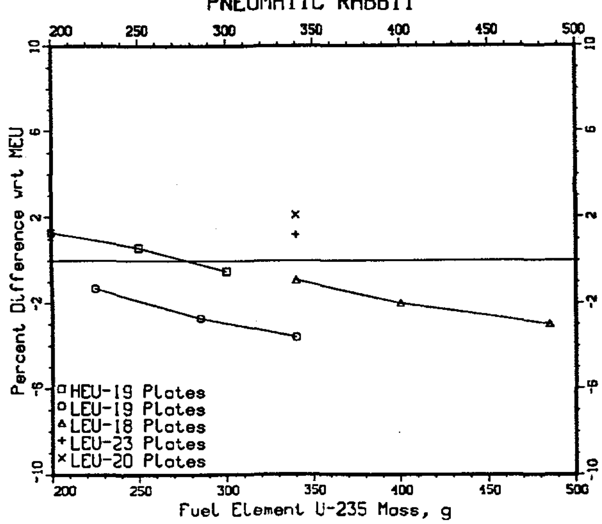

Figure 14. THERMAL-TO-TOTAL FLUX RATIO:
PNEUMATIC RABBIT

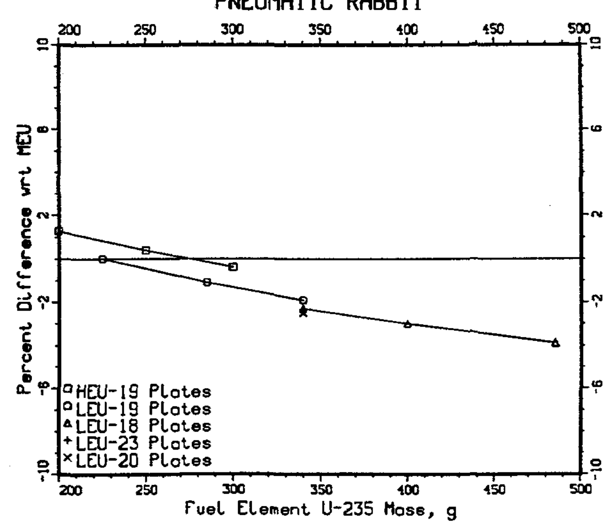

From the results it can be seen that independent of the enrichment of the fuel, increasing the uranium content in the fuel assemblies leads to lower thermal fluxes and a harder spectrum in the core while the fast flux remains relatively constant. Increasing the uranium content also results in an increase in the power densities of the peripheral fuel assemblies thus increasing the leakage from the core. The fluxes at the centre of the SILIRAD facility in the pool side are higher than at present for most of the fuels due to the increased leakage. The fluxes at this position depend solely on the fast neutron leakage while the neutron flux spectrum at this position is practically unchanged for the different fuels. This is important since irradiation damage to the silicon ingots is dependent on the neutron flux spectrum.

Changing the number of fuel plates (and their meat thickness) per assembly also has the effect of changing the spectrum. Since the irradiation positions are located either amongst the peripheral fuel assemblies or outside the core they are all directly influenced by the neutron leakage from the core. Those irradiation positions closer to the core are naturally also effected by the leakage spectrum.

It is generally known that HEU will provide a better core performance than a fuel with lower enrichment. For the sake of comparison, the performance of the irradiation positions have been compared on the basis of equal cycle lengths for two HEU versus LEU cases. The first case is a comparison between the 19-plate assembly for HEU 200 g versus LEU 225 g while the second case compares the 19-plate HEU 300 g assembly versus the 18-plate LEU 340 g assembly. Note that in these comparisons the cycle length in each case is not exactly the same; the LEU cases are some 7% longer than those of the HEU. This is not expected to have an appreciable effect on the comparison which is made in Table 5 below.

Table 5: Comparison Irradiation Facilities for HEU and LEU Fuels with Similar Cycle Lengths (LEU percentage differences from HEU)

Position	Percentage difference in thermal flux		Percentage difference in thermal-to-total ratio	
	200 g HEU vs 225 g LEU	300 g HEU vs 340 g LEU	200 g HEU vs 225 g LEU	300 g HEU vs 340 g LEU
Pool Side	- 3.0	- 3.2	0.0	0.0
Neutron Radiography Beam Tube	- 4.8	- 4.4	- 1.0	- 1.3
Molybdenum	- 4.3	- 2.9	- 2.4	- 3.6
Hydraulic Rabbit	- 5.2	- 4.5	- 2.3	- 3.3
Pneumatic Rabbit Vicinity	- 2.6	- 0.5	- 1.3	- 1.9

The maximum effect on the irradiation positions of the LEU versus HEU fuel in the above comparison is a reduction in the thermal flux of just over 5% and a hardening of the spectrum by just under 4%.

CONCLUSION

A wide range of fuel loadings, uranium enrichments and assembly geometries applicable to SAFARI-1 have been studied. The results provide a neutronic overview of SAFARI-1's current operation as well as its future operation. The impact of fuelling SAFARI-1 with LEU silicide fuel has been shown both from the points of view of the fuel economy and the performance of all major irradiation positions. It is now necessary to perform the safety and overall economic impact studies.

The cycle length and the number of assemblies used annually can be matched with a maximum of just over 5% reduction in the average thermal flux accompanied by a 4% hardening of the average flux spectrum in the irradiation facilities. Although the number of LEU assemblies used will be the same as that of HEU approximately 10% more uranium-235 would be required for the manufacture of the LEU fuel assemblies due to their larger loading.

The following example defines an envelope into which all the calculational results presented in this paper fall. If, for example, the U^{235} content per assembly is increased to 485 g with LEU silicide fuel, it is possible to reduce the current number of MEU fuel assemblies used per year by a factor of almost three. Performance in the irradiation facilities shows a maximum 10% reduction in the thermal flux and 10% hardening of the spectrum; the performance in the pool side shows a 10% increase in the thermal flux with no change in the thermal-to-total flux ratio.

ACKNOWLEDGEMENT

The authors wish to thank the staff of the RERTR Program at ANL and the Applied Radiation Technology Program at the AEC for their invaluable advice and assistance.

REFERENCES

[1] P.A. Louw, D.G. Robertson, W.J. Strydom, "Neutron Transmutation Doping in the SAFARI-1 Research Reactor", Proceedings of the 9th Pacific Basin Nuclear Conference, Sidney, Australia, 1-6 May 1994.

[2] M.M. Bretscher, "Testing WIMSD4m Cross Sections and the ANL ENDF/B-V 69-Group Library: Results from Global Diffusion and Monte Carlo Calculations Compared with Measurements in the Romanian 14-MW TRIGA Reactor", JAERI-M 94-042, (March 1994)

[3] B.J. Toppel, "User's Guide for the REBUS-3 Fuel Cycle Analysis Capability", ANL-83-2 (March 1983)

[4] K.L. Derstine, "DIF3D: A Code to Solve One-, Two-, and Three-dimensional Finite-Difference Diffusion Theory Problems", ANL-82-64, (April 1984)

[5] "MCNP4A: Monte Carlo N-Particle Transport Code System", Los Alamos National Laboratory, CCC-200, (March 1994)

APPENDIX

Fuel Shuffle Scheme for Equilibrium Cycles

Cycle	Fuel Path 1	Fuel Path 2	Fuel Path 3	Control Path 1	Control Path 2
1	H3	H7	B3	G7	C7
2	H6	G8	H4	G7	C7
3	B7	B4	H5	G7	C7
4	D3	G4	E8	G7	C7
5	F3	B5	B6	C5	E7
6	D7	F7	G6	C5	E7
7	C4	D4	C6	C5	E7
8	F4	F6	F5	C5	E7
9	E6	D5	E4	E5	G5
10		D6		E5	G5
11				E5	G5
12				E5	G5